



Renal tubule ectopic lipid deposition in diabetic kidney disease rat model and in vitro mechanism of leptin intervention

Shasha Liu¹ · Jingjing Da^{1,2,3} · Jiali Yu^{1,2,3} · Rong Dong^{2,3} · Jing Yuan² · Fuxun Yu³ · Yan Zha^{1,2,3}

Received: 8 September 2021 / Accepted: 14 January 2022 / Published online: 22 February 2022
© The Author(s) under exclusive licence to University of Navarra 2022

Abstract

Diabetic kidney disease (DKD) is a major health burden closely related to lipid metabolism disorders. Leptin has lipid-lowering efficacy, but the specific mechanism of its local effects on kidney is still unclear. This study aims to investigate the role of ectopic lipid deposition (ELD) in DKD and evaluate the lipid-lowering efficacy of leptin in the palmitic acid (PA)-induced renal tubular epithelial cells (NRK-52E). DKD model was established in *Sprague–Dawley* (SD) rats by giving single intraperitoneal injection of streptozotocin (STZ, 30 mg/kg) after high-fat diet for 8 weeks. Then, the expression changes of lipid metabolism-related markers were observed. At week 12, the protein expression level of lipid-deposited marker adipose differentiation-related protein (ADRP) was significantly increased. Besides, the lipid synthesis marker sterol regulatory element-binding protein 1c (SREBP 1c) was highly expressed while the expression of insulin-induced gene 1 (Insig-1), a key molecular of inhibiting SREBP 1c, was decreased. Leptin and compound c were incubated with the PA-induced NRK-52E cells to investigate the lipid-lowering effects and whether this effect was mediated by the AMPK/Insig-1/SREBP 1c signaling pathways. mRNA and protein of ADRP and SREBP 1c were reduced after leptin treatment, while Insig-1 and phosphorylated AMP-activated protein kinase (AMPK) were increased. Conversely, inhibition of AMPK phosphorylation by compound c mostly eliminated lipid-lowering efficacy of leptin in PA-induced cells. Collectively, these results suggested that there was ELD of renal tubular epithelial cells in DKD rats. Leptin upregulated the expression level of Insig-1 by activating AMPK to attenuate ELD in PA-induced NRK-52E cells.

Keywords Diabetic kidney disease · Ectopic lipid deposition · Leptin · Insulin-induced gene 1 · AMP-activated protein kinase

Key Points

1. Lipid deposition was increased in renal tissues of DKD rats.
2. Abnormal expression of Insig-1 may be involved in renal lipid deposition.
3. Leptin attenuated lipid accumulation in PA-induced NRK-52E cells.
4. Leptin increased Insig-1 activity by the activation of AMPK phosphorylation.

✉ Yan Zha
yanzhagz@126.com

¹ School of Medicine, Guizhou University, Guiyang 550025, Guizhou, China

² Department of Nephrology, Guizhou Provincial People's Hospital, 83, Zhongshan Road, Nanming District, Guiyang 550002, Guizhou, China

³ NHC Key Laboratory of Pulmonary Immunological Disease, Guizhou Provincial People's Hospital, Guiyang 550002, Guizhou, China

Introduction

Diabetes mellitus (DM) is associated with a variety of complications, such as retinopathy, nephropathy, and diabetic ketoacidosis (DKA) [9, 30]. Diabetic kidney disease (DKD) is a major microvascular complication of DM, and eventually leads to end-stage renal disease (ERSD) [10, 33]. It is reported that type 2 diabetic nephropathy (T2DN) rats developed renal and physiological abnormalities similar to clinical observations in human patients with DKD, indicating T2DN rat is an excellent model for studying the progression of renal damage in DKD [27]. Emerging studies found lipid accumulation in the renal tissues of diabetes patients and experimental animal models, which indicated that DN is associated with ectopic lipid deposition (ELD) [16, 31, 37]. ELD is the excessive accumulation of lipid in non-adipose tissue, leading to lipotoxic damage of non-adipose cells [19, 40]. Recently, it has been documented that the renal tubular

injury plays an integral role in the pathogenesis of DKD [41], and suggested that ELD is related to renal tubule injury in DKD [39], but the specific mechanism is still unclear.

Vaziri reported that lipid and lipoprotein metabolism disorders are closely related to the development and progression of kidney diseases [34]. Studies have shown that adipose differentiation-related protein (ADRP) is located on the surface of lipid droplets and is the main component of lipid droplet vesicle formation in cells. It plays a pivotal role in the balance between cellular lipid storage and lipid outflow; thus, its increased expression may suggest a specific marker for lipid deposition [3, 4]. Eberlé et al. [7] and Sun et al. [32] suggested that sterol regulatory element-binding protein (SREBP) transcription factors serve a family of transcription factors which regulate lipid homeostasis by controlling cellular fatty acid, triacylglycerol, and cholesterol synthesis. It has been demonstrated that SREBP-1 protein levels are significantly increased in the kidneys of type 2 diabetic animals and reducing the expression of SREBP-1 in diabetic kidney can delay the progression of the kidney [18, 31]. Insulin-induced gene 1 (Insig-1) is a new regulatory factor of lipid metabolism, which is widely involved in the regulation of intracellular lipid metabolism, and the abnormal expression of Insig-1 is involved in various lipid disorders [26]. Served as a potent inhibitor for the proteolytic process and maturation of SREBP by binding the sterol-sensing domain of SREBP cleavage-activating protein (SCAP), Insig-1 facilitates retention of the SCAP/SREBP complex in the endoplasmic reticulum (ER) [38]. It has been reported that overexpression of Insig-1 in liver can improve hepatic steatosis [15]. These studies implied that Insig-1 might play a potential role in the pathogenesis of ELD in DKD.

Leptin, a 167-amino acid adipokine, plays a critical role in regulating body weight, food intake, and energy metabolism [42]. It has been reported that insulin resistance and hepatic steatosis are improved in some patients with lipodystrophy after receiving leptin replacement therapy [28]. Besides, leptin is a key factor in regulating lipid metabolism. Diéguez et al. [6] revealed that leptin treatment stimulated the lipolytic action in the adipose tissues, and the activation of AMPK in skeletal muscle could protect non-adipocytes from lipotoxicity. AMP-activated protein kinase (AMPK) is a metabolic sensor in mammals, which modulates lipid metabolism by directly phosphorylating proteins or modulating gene transcription in specific tissues [36]. It has been reported that leptin is thought to be metabolized primarily by the kidney and is bound and absorbed by megalin in the proximal convoluted tubules [14]. Megalin was a large glycosylated receptor belonging to the low-density lipoprotein receptor family. It is partly located in the microvilli of proximal tubule epithelial cells (PTECs) and plays a key role in the reabsorption of diverse glomerular-filtered substances, including albumin and low molecular weight proteins [20,

25]. Thus, leptin could reduce lipid accumulation in non-adipose tissue, but its role in the kidney is unclear.

Therefore, the present study aims to observe the changes of lipid deposition-related proteins in T2DN rat model and investigate the mechanism of leptin on lipid accumulation in PA-induced NRK-52E cells. Then, whether leptin attenuate ELD by regulating AMPK/Insig-1/SREBP 1c signaling pathways was further explored using AMPK inhibitor. The current study would provide a new strategy for the lipid metabolism regulation of leptin on the pathogenesis of DKD.

Materials and methods

Animals

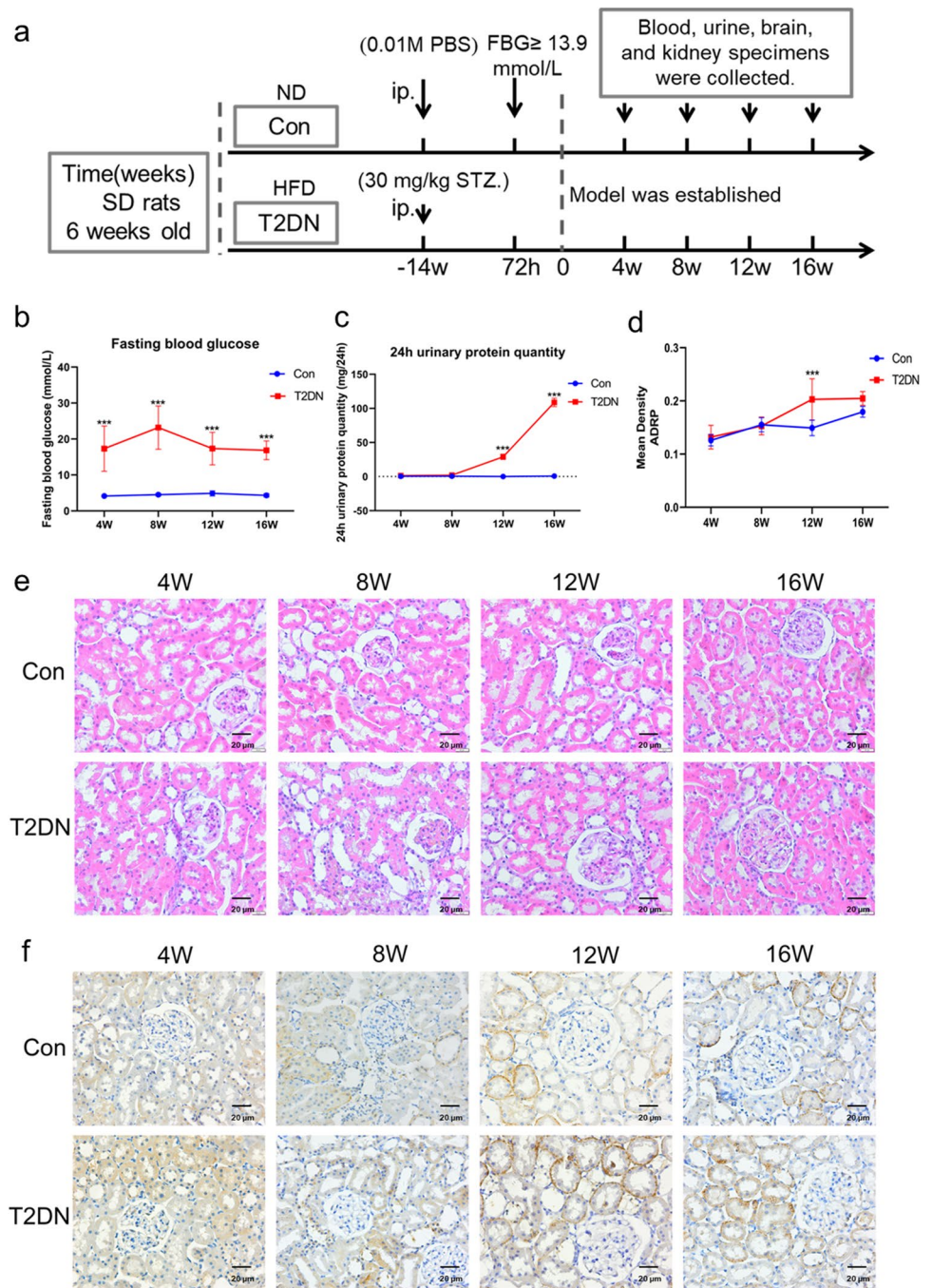
Sixty specific pathogen-free 6-week-old male *Sprague–Dawley* (SD) rats (200 ± 20 g, SCXK (Jing) 2019–0008) were purchased from Beijing Huafukang Biotechnology Co., Ltd. (Beijing, China). Rat experiments were conducted in accordance with the policies of the National Institutes of Health Guidelines for the Care and Use of Laboratory Animals and China animal welfare legislation. The research was approved by the ethics committee of Guizhou People's Hospital [Approval Number: (2020)090]. The study protocol was approved by the institutional animal care and welfare committee. All animals were raised in the standard temperature ($21 \text{ }^\circ\text{C} \pm 2 \text{ }^\circ\text{C}$) and stable humidity ($55\% \pm 2\%$) with a light/dark cycle of 12/12 h. All animals were allowed to have free access to standard food and water and habituated to the animal facilities for a week. All animal experiments were done at the animal center of Guizhou Medical University.

Animal models establishment, drug administration, and grouping design

All rats were randomly assigned to two groups: control (Con) and T2DN groups. The T2DN group rats were fed a high-fat diet (HFD) for 8 weeks and the Con group rats were fed a normal diet (ND). A single dose of STZ (30 mg/kg) was intraperitoneally injected into the T2DN group rats. The Con group rats were intraperitoneally injected the same dose of normal saline. After 72 h, the tail vein blood glucose was measured. If the fasting blood glucose (FBG) ≥ 13.9 mmol/L, the T2DN model was successfully established. The animal experiment lasted for 16 weeks (Fig. 1a).

Samples' collection and indicators' detection: before measuring FBG, all rats were fasted for 12 h. Then, the vail vein blood glucose was measured using a blood glucose test chip (Roche Diabetes Care GmbH, Shanghai, China). All rats were housed in metabolic cages to collect 24-h urine, and 24-h urinary albumin was measured

Fig. 1 Comparison of renal function-related indicators, renal histopathology change, and ectopic lipid accumulation of the different group rats. **a** Timeline of the rat experiment. T2DN model was induced by a single intraperitoneal injection of streptozotocin (STZ) after a high-fat diet (HFD) for 8 weeks. Then, 4-, 8-, 12-, and 16-week specimens were collected. **b** Fasting blood glucose. **c** 24-h urinary protein quantity. **d** ADRP protein expression quantified by Integrated Performance Primitives (IPP) 6.0 software, and the results are expressed as positive integrated optical density (IOD). **e** Representative images (scale bar = 20 μ m, magnification 400 \times) of kidney sections in hematoxylin and eosin (HE). **f** Representative images (scale bar = 20 μ m, magnification 400 \times) of immunohistochemistry for ADRP. **Abbreviations:** i.p., intraperitoneal; ND, normal diet; HFD, high-fat diet; Con, control; T2DN, type 2 diabetic nephropathy. All values are presented as means \pm SD; *** P < 0.001 vs Con group



using a QuantiChrom™ BCG albumin assay kit (Bioassay Systems, Hayward, CA). Then, the 24-h urine volume and 24-h urinary albumin were used to calculate the 24-h urinary protein quantity. All rats were sacrificed with 4% pentobarbital sodium (50 mg/kg, Sigma, Merck, Germany) anesthesia. Blood, urine, brain, and kidney were collected at weeks 4, 8, 12, and 16. The serum was separated and stored at -80°C . Brain and kidney tissues were stored in liquid nitrogen or 4% paraformaldehyde.

Histological examination and immunohistochemistry of renal tissues

Harvested kidneys were immersion fixed (4% paraformaldehyde), embedded in paraffin, and sliced into 4- μ m-thick sections. Hematoxylin and eosin (HE) staining was performed to observe the pathological and morphological changes in rat renal tissues. Immunohistochemical staining: tissue sections were dewaxed, rehydrated, and exposed to 3% H_2O_2 (10 min)

to quench the endogenous peroxidase. Antigen retrieval with 0.01 M sodium citrate buffer under high pressure and high temperature, the sections were blocked by 5% bovine serum albumin (BSA) for 30 min at room temperature (RT). The sections were then incubated with anti-SREBP 1c antibody (Sc-13551, 1:100 dilution; Dallas, TX, USA), anti-ADRP antibody (1s294-1-AP, 1:200 dilution; Proteintech, Wuhan, China), and anti-Insig-1 antibody (22,115-1-AP, 1:100 dilution; Proteintech, Wuhan, China) at 4 °C overnight. Next, the sections were washed in 0.01-M phosphate buffer saline (PBS) and then incubated with the corresponding HRP-conjugated secondary antibody (Abcam, Cambridge, UK) for 90 min at RT and 30 min at 37 °C. Subsequently, DAB kit (Zhongshan Jingqiao Biotechnology, Beijing, China) staining was used to observe protein expression. For each slice, 10 nonoverlapping fields in the cortical area were randomly selected for the measurement of the integrated optical density (IOD) using a fully automated image analysis system (Image-Pro Plus 6.0). IOD was used as a measure of the relative content of positive substances in each slice.

Cell culture

Renal tubular epithelial cells (NRK-52E; Cell Bank of Chinese Academy of Sciences, Shanghai, China) were grown in Dulbecco's modified Eagle's medium (DMEM) (ThermoFisher, Suzhou, China) supplemented with 5% heat-inactivated fetal bovine serum (FBS) (Biological Industries, Kibbutz Beit Haemek, Israel) and 1% penicillin/streptomycin (Solarbio, Beijing, China), at the condition of 37 °C, 5% CO₂, and 95% humidity. NRK-52E cells had been used in various passage numbers from 3 to 9. Cells were incubated with 0.2-mM PA and various concentrations of leptin (0.62, 6.25, 12.5 nM) for 24 h. For some experiments, cells were incubated with 0.2-mM PA for 24 h after pretreatment with or without compound c (10 μM, 30 min) (B3252, ApexBio Technology, Houston, USA) or leptin receptor antagonist (10 ng/mL, 10 min) (CB500256, California Bioscience, CA, USA). Then, cells were treated with 12.5-nM leptin for 24 h. NRK-52E cells were starved overnight in culture medium without FBS prior to treatment with PA. NRK-52E cells incubated with BSA served as controls.

Oil Red O staining

Cells grown on coverslips were first washed in PBS and fixed with 4% paraformaldehyde for 20 min, and washed thrice in PBS. Next, the cells were incubated in isopropyl alcohol (60%, v/v) for 5 min and then subjected to Oil Red O staining for 15 min, and washed thrice in PBS. The cells were counterstained with hematoxylin and then washed in PBS thrice, and images were obtained under a microscope (Olympus, Tokyo, Japan).

Cellular total triglyceride measurement

The cells were homogenized for 1 min by adding appropriate amount of PBS solution under ice water bath, and triglyceride (TG) content of the prepared homogenate was detected by a TG detection kit (Jiancheng Bioengineering Institute, Nanjing, China).

Quantitative real-time PCR (qRT-PCR)

Total RNA was extracted using TRIzol reagent (TaKaRa, Shiga, Japan) according to the manufacturer's instructions. Then, samples containing 5 μg of RNA were reverse transcribed to obtain cDNA using PrimeScript® RT reagent kit (ThermoFisher, Suzhou, China) according to the manufacturer's protocol. qRT-PCR was performed using SYBR Green Talent qPCR PreMix kit (TianGen, Beijing, China). The mRNA expression level was calculated using the comparative cycle threshold (Ct) method normalized to *GAPDH*. Specific primer sequences used for qRT-PCR are listed in Table 1.

Immunofluorescence test

Prior to treatment, NRK-52E cells were seeded on glass coverslips, washed in PBS, and fixed for 20 min in 4% paraformaldehyde. Cells were blocked in normal donkey serum (Solarbio, Beijing, China) for 1 h, and incubated overnight at 4 °C with primary antibody against ADRP (1s294-1-AP, 1:200 dilution; Proteintech, Wuhan, China). After washing with PBS, cells were incubated with Alexa Fluor 488-conjugated secondary antibodies (ab150073, 1:100 dilution; Abcam, Cambridge, UK) for 2 h at RT and counterstained

Table 1 Sequences of the primers for qRT-PCR

Genes	Sequence (5' to 3')	Annealing temperature, °C
<i>GAPDH</i>	F: CAAGGTACTCCATGACAACCTTTG	60
	R: GGGCCATCCACAGTCTTCTG	
<i>AMPK</i>	F: GCCGAGAAGCAGAAGCACGAC	60
	R: GCTTGCCACCTTCACTTTCCC	
<i>Insig-1</i>	F: CTCCCGCGAGGCATGATT	60
	R: CGCCAAATGAGAAGAGCACG	
<i>SREBP 1c</i>	F: CGCTTCTTACAGCACAGCAA	60
	R: TGCCCAAGGACAAGGGGCTA	
<i>ADRP</i>	F: AGCTCCACTCCACTGTCCATCTG	60
	R: TAGCCGACGATTCTTCCACTCC	

F, forward primer; R, reverse primer; *AMPK*, AMP-activated protein kinase; *Insig-1*, insulin-induced gene 1; *SREBP 1c*, sterol regulatory element-binding protein 1c; *ADRP*, adipose differentiation-related protein. *GAPDH* as reference genes.

with DAPI for 15 min. Coverslips were visualized using an Olympus BX53 fluorescence microscope and photographed with Cellsens Entry software (Olympus, Tokyo, Japan).

Western blotting

Cells were lysed in RIPA buffer (Solarbio, Beijing, China) containing 1% PMSF (Solarbio, Beijing, China) and 1% protease inhibitor cocktail (Solarbio, Beijing, China). The supernatant was obtained and protein content was determined by bicinchoninic acid protein assay kit (Solarbio, Beijing, China). Samples containing 20 µg of protein were separated by 10% sodium dodecyl sulfate–polyacrylamide gel electrophoresis and transferred to a polyvinylidene difluoride (PVDF) membrane (Immobilon-P, 0.45 µm, Merck Millipore, Darmstadt, Germany). The membranes were blocked in 5% BSA or 5% nonfat milk for 2 h, and incubated with the primary antibodies against AMPK (ab131512, 1:500 dilution; Abcam, London, UK), p-AMPK (ab194920, 1:500 dilution; Abcam), SREBP 1c (Sc-13551, 1:500 dilution; Dallas, TX, USA), Insig-1 (22,115–1-AP, 1:500 dilution; Proteintech, Wuhan, China), ADRP (1s294-1-AP, 1:500 dilution; Proteintech), and GAPDH (60,004–1-Ig, 1:3000 dilution; Proteintech). After incubating with the corresponding HRP-conjugated secondary antibody (Abcam, Cambridge, UK) at 37 °C for 2 h, the protein samples were detected by ECL reagents (Millipore, Billerica, MA) and quantification of signals was performed using ImageJ software (Rawak Software Inc., Stuttgart, Germany).

Statistical analysis

All statistical analyses were performed using the GraphPad Prism (8.0.2. for Windows, GraphPad Software, San Diego, CA, USA). All experiment data were expressed as the means ± SD. The means were compared using Student's *t*-test or one-way ANOVA of variance. *P* values < 0.05 were considered statistically significant.

Results

Ectopic lipid accumulation of renal tubular epithelial cells in T2DN rats

Six-week-old SD rats were fed with HFD for 8 weeks and a single intraperitoneal injection of STZ to induce the T2DN model. To determine whether the T2DN model had been established, the fasting blood glucose (FBG) and urinary albumin levels were tested. The FBG levels of the T2DN group in different stages (19.34 ± 4.37 mmol/L; 23.17 ± 6.01 mmol/L; 17.34 ± 4.53 mmol/L; 16.85 ± 2.59 mmol/L) were significantly higher than those

in the Con group (4.15 ± 0.39 mmol/L; 4.50 ± 0.35 mmol/L; 4.87 ± 0.72 mmol/L; 4.32 ± 0.50 mmol/L) (Fig. 1b). Compared with the Con group, the 24-h total urinary protein quantity of the T2DN group was increased (Fig. 1c). HE staining showed that the kidney tissues of T2DN groups had glomerular hypertrophy and mesangial matrix expansion, and some renal tubular epithelial cells showed vacuolar degeneration and partial shedding (Fig. 1e). These results demonstrated that the T2DN model was successfully established.

In order to detect lipid deposition of kidney tissues in T2DN rats, immunohistochemistry was used to determine the expression level of lipid-related marker (ADRP). As shown in Fig. 1d and f, compared with the Con group, the protein expression of ADRP was increased in the T2DN group, and the difference was statistically significant at the 12th week (*P* < 0.05). These data suggested that there was significant lipid deposition in the kidneys of T2DN rats at the 12th week.

Insig-1 was downregulated in T2DN rats

Next, we investigated whether Insig-1 and SREBP 1c were involved in lipid deposition of T2DN rats. The Insig-1 and SREBP 1c expression levels in kidney were detected by immunohistochemistry. As shown in Fig. 2a and b, compared with the Con group, protein expression level of SREBP 1c was increased in the T2DN group. Interestingly, as shown in Fig. 2a and c, the expression level of Insig-1 of kidneys in the T2DN group was significantly lower than that in the Con group. These results indicated that lipid deposition in the T2DN group was related to the decrease of Insig-1 and the increase of SREBP 1c, which may play a key role in the regulation of renal lipid metabolism in T2DN rats.

Leptin attenuated lipid accumulation in PA-induced NRK-52E cells

NRK-52E cells were incubated with 0.2-mM PA for 24 h to induce lipid accumulation, and different concentrations of leptin (0.62, 6.25, 12.5 nM) were added for 24 h. Lipid deposition in PA-induced NRK-52E cells, and leptin attenuated lipid accumulation were observed after Oil Red O Staining (Fig. 3a). Consistent with the Oil Red O staining results, compared with the Con group, TG content was significantly increased in PA-induced cells, and 0.62-, 6.25-, and 12.5-nM leptin reduced the PA-induced TG content, while the higher 2 doses had statistically significant difference (Fig. 3b). The mRNA and protein levels were detected by qRT-PCR and Western blot analysis; the expression of *ADRP* mRNA and protein in the PA group was significantly higher than that in the Con group, while decreased after 6.25-nM and 12.5-nM leptin treatment

Fig. 2 Expression of lipid-related proteins in renal tissues. **a** representative images (scale bar = 20 μ m, magnification 400 \times) of immunohistochemistry for SREBP 1c and Insig-1. **b, c** SREBP 1c and Insig-1 protein expression quantified by Integrated Performance Primitives (IPP) 6.0 software, and the results are expressed as positive integrated optical density (IOD). **Abbreviations:** Con, control; T2DN, type 2 diabetic nephropathy. All values are presented as means \pm SD; * P < 0.05, ** P < 0.01 vs Con group

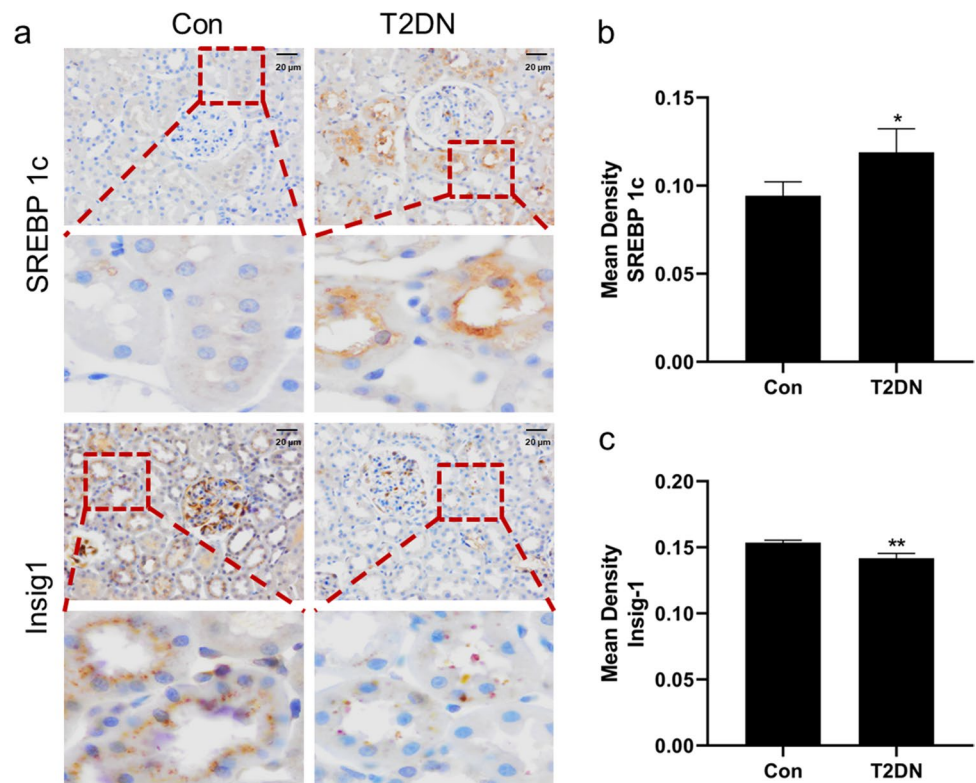


(Fig. 3c, d, e). Taken together, these data indicated that leptin attenuated PA-induced lipid accumulation in NRK-52E cells.

Leptin upregulated *Insig-1* and downregulated lipid synthesis gene expression in PA-induced NRK-52E cells

Next, we examined whether leptin can regulate *Insig-1* and inhibit the expression of lipid synthesis gene. The expression of *Insig-1* and lipid synthesis gene were detected by qRT-PCR, compared with the PA group and mRNA levels of *Insig-1* were increased after 12.5-nM leptin treatment, while mRNA levels of *SREBP 1c* were significantly decreased, but levels of *AMPK* were not changed (Fig. 4a, b, c). Consistent with the qRT-PCR results, the protein expression level of SREBP 1c was decreased after leptin treatment in PA-induced NRK-52E cells (Fig. 4d, g). Compared with the PA group, the protein expression of *Insig-1* and the p-AMPK/AMPK ratio were obviously increased after the treatment of leptin, while the higher 2 doses had statistically significant difference (Fig. 4d, e, f). Together, these data indicated that leptin increased AMPK phosphorylation levels and upregulated *Insig-1*, whereas inhibited the expression of lipid synthesis gene SREBP 1c and attenuated lipid deposition in PA-induced NRK-52E cells.

Leptin improved lipid deposition in PA-induced NRK-52E cells by enhancing AMPK phosphorylation

It is reported that activation of AMPK enhanced *Insig-1* expression and improved hepatic steatosis in HFD mice [15]. Therefore, NRK-52E cells were incubated with 0.2-mM PA and 10- μ M AMPK inhibitor (compound c, Cc) or 10 ng/mL leptin receptor antagonist (I). Western blot analysis was used to determine the effects of compound c on p-AMPK/AMPK; as shown in Fig. 5c and d, the ratio of p-AMPK/AMPK was decreased. Compared with the leptin treatment (the PA + lep group), Oil Red O staining showed that inhibiting AMPK led to the increase of the lipid content, but the lipid content not obviously increased in the receptor antagonist-treated group (the PA + lep + I group) (Fig. 5a). Consistent with the Oil Red O staining results, the TG content in the AMPK inhibitor group (the PA + lep + Cc group) was higher than that in the PA + lep group; the difference was statistically significant (Fig. 5b). Similarly, the expression of lipid-related marker ADRP was increased after adding compound c detected by immunofluorescence test and Western blot analysis (Fig. 5a, c, g).

However, compared with the PA + lep group, the protein expression of ADRP seemed to be not changed in the PA + lep + I group by immunofluorescence test and Western blot analysis (Fig. 5a, c, g), and the TG content was consistent with the ADRP expression result (Fig. 5b). As shown in

Fig. 3 Effects of leptin on lipid accumulation in PA-induced NRK-52E cells. **a** Intracellular lipid content was detected by Oil Red O staining (scale bar = 20 μ m, magnification 400 \times). **b** TG content in different groups. **c** ADRP mRNA detected by qRT-PCR. **d** Effects of leptin on the expression of ADRP protein in NRK-52E cells. NRK-52E cells were treated with a 0.2-mM PA and different concentrations of leptin (0.62, 6.25, 12.5 nM) for 24 h, measured by Western blot analysis, GAPDH used as a loading control. **e** ADRP protein expression level quantified by ImageJ software. **Abbreviations:** Con, control; PA, 0.2-mM palmitic acid; PA + lep 0.62 nM, 0.2-mM palmitic acid + 0.62-nM leptin; PA + lep 6.25 nM, 0.2-mM palmitic acid + 6.25-nM leptin; PA + lep 12.5 nM, 0.2-mM palmitic acid + 12.5-nM leptin. All values are presented as means \pm SD; ** P < 0.01, *** P < 0.001 vs Con group; # P < 0.05, ## P < 0.01 vs PA group

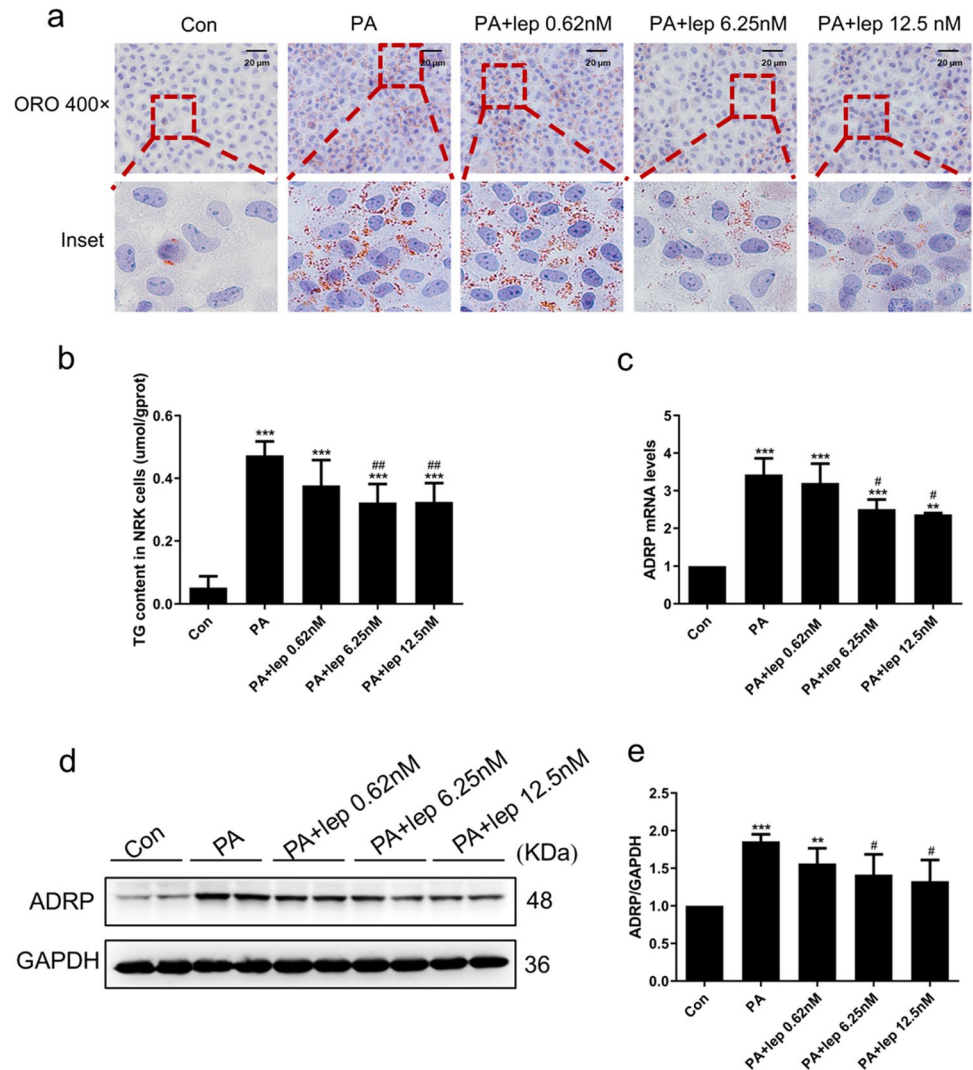


Fig. 5c, e, and f, compared with the PA + lep group, inhibition of AMPK by adding compound c reduced the protein expression of Insig-1 and increased the protein expression of SREBP 1c. The leptin receptor antagonist did not reduce these lipid-lowering effects of leptin. Together, these data suggested that AMPK was sufficient to stimulate Insig-1 activity in vitro likely through a post-translational regulation and that leptin-attenuated PA-induced lipid accumulation in NRK-52E cells may not entirely through the leptin receptor.

Discussion

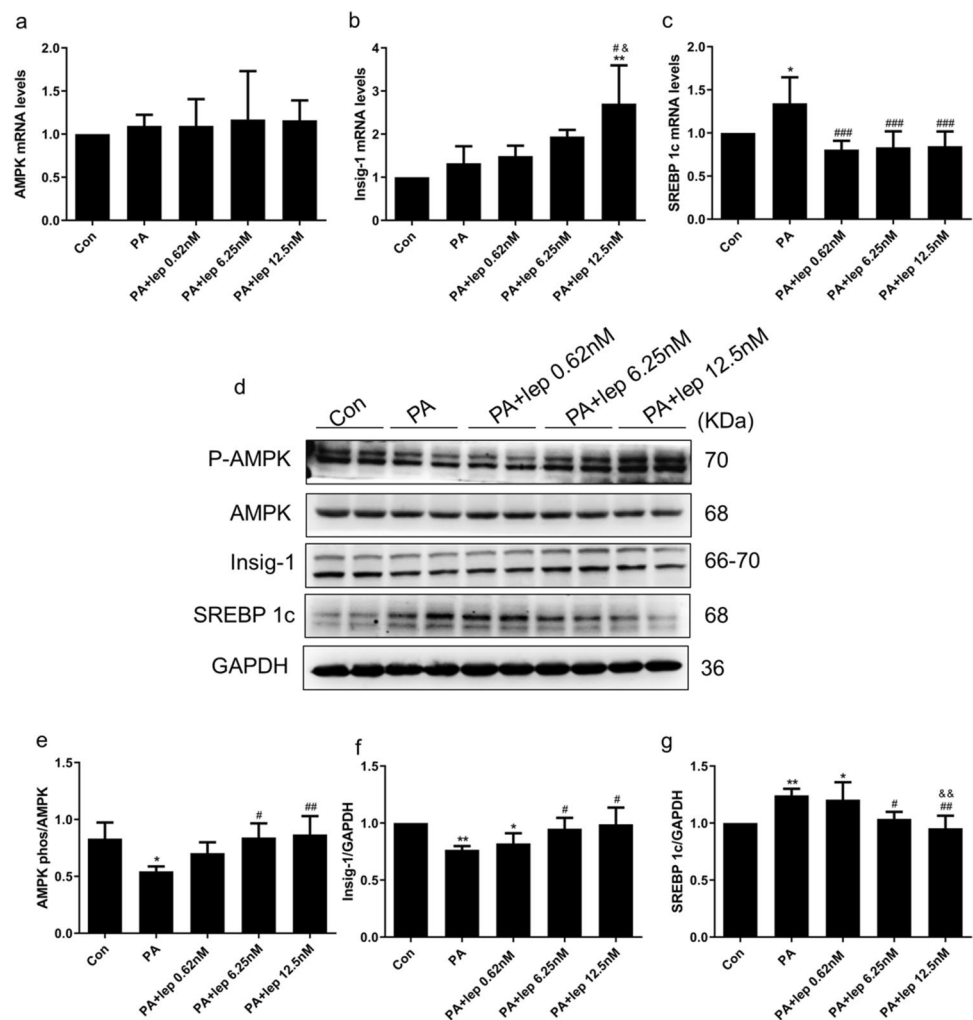
In this study, it was demonstrated that there was significant lipid deposition in the kidney of T2DN rats, the protein expression level of lipid-related marker (ADRP) was increased, and abnormal expression of SREBP 1c and Insig-1 was related to lipid synthesis. We found that leptin attenuated lipid accumulation in PA-induced NRK-52E cells

by upregulating Insig-1 through activating phosphorylation of AMPK.

Recent studies have reported that ELD occurs in non-adipose tissue and will trigger the lipotoxicity [11, 22, 31]. ELD may mediate tubular damage in DKD, ultimately leading to DN progression. It is reported that lipid deposition was observed in the kidneys of type 2 DKD patients [39], and Mishra et al. [24] also found lipid deposition in renal tissues of db/db mice by Oil Red O staining. Studies have shown that ADRP is located on the lipid droplet surface, and its expression was related to the degree of lipid accumulation, which could be used for the quantitative analysis of lipid deposition [2]. In this study, we found that the expression level of ADRP was increased in the T2DN group (Fig. 1), suggesting lipid deposition in the kidneys of T2DN rats, which is consistent with previous studies.

Herman-Edelstein et al. [16] reported that lipid deposition was associated with dysregulation of lipid metabolism genes. SREBPs belong to a family of transcription factors

Fig. 4 Effects of leptin on lipid-related proteins in PA-induced NRK-52E cells. **a–c** AMPK, Insig-1, and SREBP 1c mRNA detected by qRT-PCR. **d** Western blot analysis of the expression level of p-AMPK, AMPK, Insig-1, and SREBP 1c in NRK-52E cells, treated with a 0.2-mM PA and different concentrations of leptin (0.62, 6.25, 12.5 nM) for 24 h. **e–g** p-AMPK/AMPK, Insig-1, and SREBP 1c protein expression level measured by ImageJ software. **Abbreviations:** Con, control; PA, 0.2-mM palmitic acid; PA + lep 0.62 nM, 0.2-mM palmitic acid + 0.62-nM leptin; PA + lep 6.25 nM, 0.2-mM palmitic acid + 6.25-nM leptin; PA + lep 12.5 nM, 0.2-mM palmitic acid + 12.5-nM leptin. All values are presented as means \pm SD; * $P < 0.05$, ** $P < 0.01$ vs Con group; # $P < 0.05$, ## $P < 0.01$, ### $P < 0.001$ vs PA group; & $P < 0.05$, && $P < 0.01$ vs PA + lep 0.62 nM group



that is critical for maintaining lipid homeostasis, and it is involved in fatty acid (FA) synthesis and insulin-induced glucose metabolism in lipogenesis [7, 35]. Saravanan et al. [29] found that the expression of SREBP-1c was increased in renal tissues of HFD-induced diabetic C57BL/6 J mice. It has been reported that Insig-1 is an upstream regulatory factor of SREBP 1c, and the overexpression of Insig-1 inhibits SREBP 1c expression, thereby reducing insulin-stimulated lipogenesis in the livers of transgenic mice [8]. Han et al. [15] also reported that increasing the stability of Insig-1 can reduce the expression of lipogenic genes and attenuate hepatic steatosis in HFD-induced mice. These studies suggested that Insig-1 plays a key role in the regulation of ELD. Therefore, we speculated that the abnormal expression of Insig-1 protein may lead to lipid deposition in T2DN rats. Our results demonstrated that the expression level of SREBP 1c was significantly increased, while the expression level of Insig-1 was decreased in the T2DN rat model (Fig. 2). These results suggested that Insig-1 may also as a potential target for the treatment of lipid deposition in T2DN rat model.

Leptin is an adipocyte-derived hormone with both central and peripheral effects on energy metabolism. Study has reported that leptin targets the hypothalamus to protect from steatosis by promoting hepatic triglyceride export and decreasing lipogenesis independent from caloric intake [13]. However, there is no evidence related to the effect of leptin on renal lipid deposition. Leptin has been suggested to be primarily metabolized by the kidneys, taken up by proximal convoluted tubules and where megalin likely mediates its binding and uptake [14]. Although growing studies focus on that leptin resistance, it has been shown that high concentrations of leptin have pro-inflammatory and pro-apoptotic effects on the kidneys [1, 5, 17]. However, it has also been reported that leptin can attenuate apoptotic injury in gentamicin-induced NRK-52E cells through PI3K/Akt signaling pathway [5]. Leptin itself can promote lipolysis and inhibit lipid synthesis [23], but the role of leptin in high lipid-induced renal tubular epithelial cells is unclear. In this study, we observed that leptin can reduce the expression of ADRP in PA-induced NRK-52E cells, suggesting its lipid-lowering effect (Fig. 3).

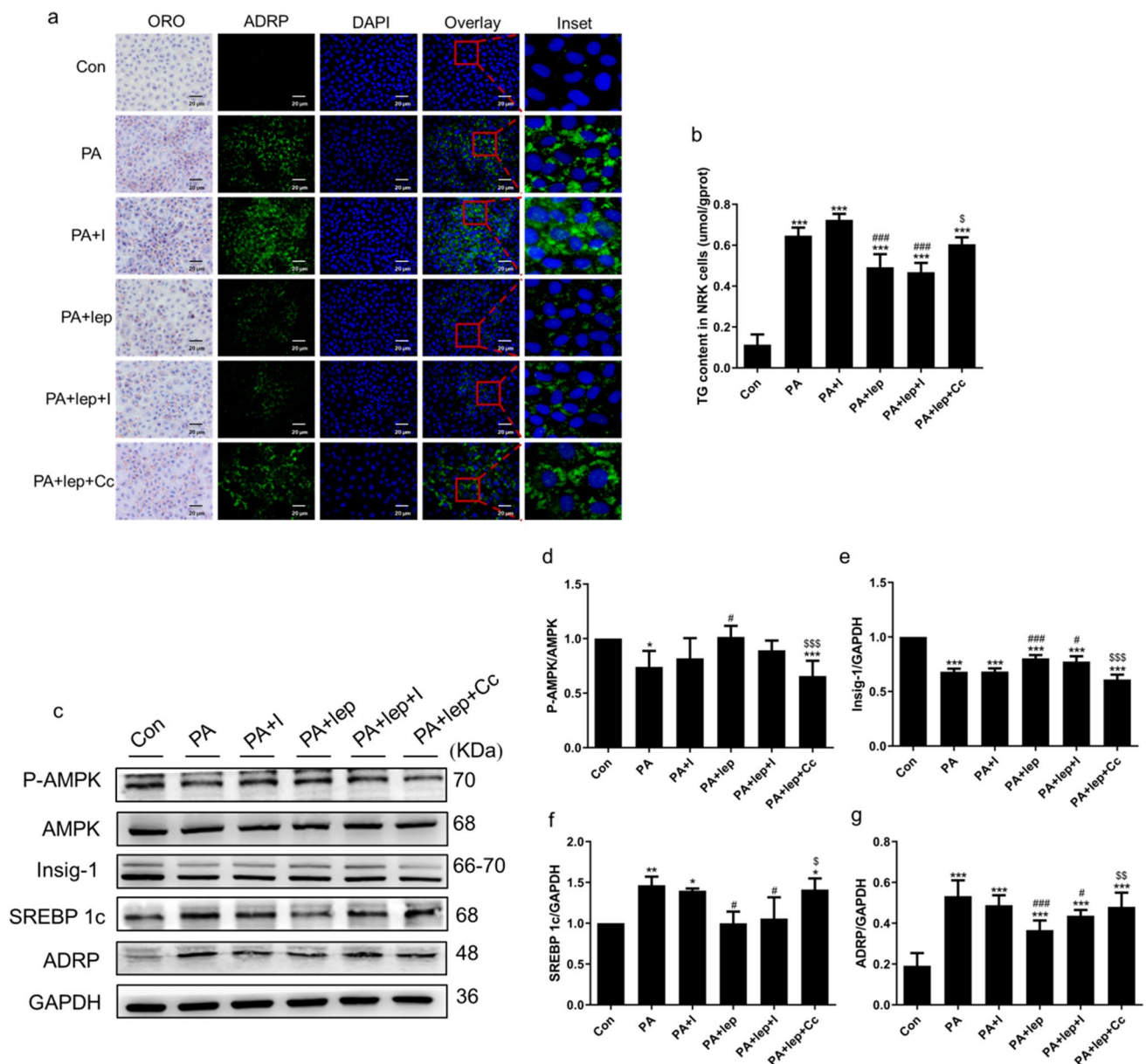


Fig. 5 Leptin upregulated Insig-1 expression by the activation of AMPK and inhibits lipid synthesis in PA-induced NRK-52E cells. **a** Intracellular lipid content was detected by Oil Red O staining (scale bar=20 μ m, magnification 400 \times) and representative images of immunofluorescence for ADRP protein expression in NRK-52E cells (scale bar=20 μ m, magnification 400 \times). **b** TG content in different groups. **c** Representative Western blot analyses of p-AMPK, AMPK, Insig-1, SREBP 1c, and ADRP protein expression in NRK-52E cells treated with or without 0.2-mM PA in the presence or absence of 12.5-nM leptin and pretreatment with or without 10- μ M compound c or 10 ng/mL leptin receptor antagonist, GAPDH used

as a loading control. **d-g** p-AMPK/AMPK, Insig-1, SREBP 1c, and ADRP protein expression level quantified by ImageJ software. **Abbreviations:** Con, control; PA, 0.2-mM palmitic acid; PA+I, 0.2-mM palmitic acid+10 ng/mL leptin receptor antagonist; PA+lep, 0.2-mM palmitic acid+12.5-nM leptin; PA+lep+I, 0.2-mM palmitic acid+12.5-nM leptin+10 ng/mL leptin receptor antagonist; PA+lep+Cc, 0.2-mM palmitic acid+12.5-nM leptin+10- μ M compound c. All values are presented as means \pm SD; * P <0.05, ** P <0.01, *** P <0.001 vs Con group; # P <0.05, ### P <0.001 vs PA group; ^s P <0.05, ^{SS} P <0.01, ^{SSS} P <0.001 vs PA+leptin group

AMP-activated protein kinase (AMPK) is a serine/threonine protein kinase that emerges as a sensor of cellular energy [12]. In eukaryotes such as mammals, AMPK is believed to act as a key master switch that modulates lipid metabolism by directly phosphorylating proteins or

modulating gene transcription in specific tissues such as the liver, fat, and muscle [36]. Li et al. [21] reported that AMPK activation can inhibit SREBP-1c cleavage and nuclear translocation, thereby reducing lipogenesis and lipid accumulation in hepatocytes induced by high glucose. Other studies

have shown that activation of AMPK can enhance Insig-1 expression and lead to improvement of hepatic steatosis in HFD-induced mice [15]. Our findings confirmed that leptin reduced the expression of lipid synthesis genes, and increased Insig-1 expression (Fig. 4). Furthermore, our study further identified that leptin upregulated Insig-1 by the activation of AMPK (Fig. 5), suggesting leptin could attenuate lipid deposition by regulating AMPK/Insig-1/SREBP 1c pathway.

There are some limitations in this study. First, although *in vivo* and *in vitro* methods were used in this study, Oil Red O staining is needed to further verify lipid accumulation in T2DN rats. Then, although we showed that leptin-improved lipid accumulation may not entirely through the leptin receptor, but we could not identify the other receptors leptin may bind. Therefore, the specific mechanism of leptin receptor remains to be further studied.

In conclusion, we demonstrated that there was lipid deposition in the kidney of T2DN rats with the mechanism of increasing SREBP 1c protein expression and decreasing Insig-1 protein expression. Leptin attenuated lipid deposition by activating AMPK phosphorylation which upregulated the expression of Insig-1 in PA-induced NRK-52E cells.

Author contribution Conceptualization: Shasha Liu; data acquisition: Shasha Liu and Jingjing Da; methodology: Jiali Yu and Rong Dong; resources: Yan Zha and Fuxun Yu; data curation: Shasha Liu and Jingjing Da; writing, review, and editing: Shasha Liu, Jingjing Da, Yan Zha, and Jing Yuan; visualization: Jiali Yu and Rong Dong; supervision: Yan Zha, Jing Yuan, and Fuxun Yu; project administration and funding: Yan Zha, Jingjing Da, and Jing Yuan. The authors declare that all data were generated in-house and that no paper mill was used.

Funding This work was supported by the National Natural Science Foundation of China (Grants No. 81760134, 81960139), and Guizhou Science and Technology Department (Grants No. QKHP-TRC2018-5636, QKHZC2019-2801, QKHPTRC2020-2201, QKHJC2020-1Y304, and QKHJC2019-1194). National Natural Science Foundation of China, 81760134, Yan Zha, 81960139, Jingjing Da, Guizhou Science and Technology Department, QKHPTRC2018-5636, Yan Zha, QKHZC2019-2801, Yan Zha, QKHPTRC2020-2201, Yan Zha, QKHJC2020-1Y304, Jingjing Da, QKHJC2019-1194, Jing Yuan

Declarations

Conflict of interest The authors declare no competing interests.

References

- Alhasson F, Seth RK, Sarkar S, Kimono DA, Albadrani MS, Dattaroy D, Chandrashekar V, Scott GI, Raychoudhury S, Nagarkatti M, Nagarkatti P, Diehl AM, Chatterjee S (2018) High circulatory leptin mediated NOX-2-peroxynitrite-miR21 axis activate mesangial cells and promotes renal inflammatory pathology in nonalcoholic fatty liver disease. *Redox Biol* 17:1–15. <https://doi.org/10.1016/j.redox.2018.04.002>
- Bickel PE, Tansey JT, Welte MA (2009) PAT proteins, an ancient family of lipid droplet proteins that regulate cellular lipid stores. *Biochem Biophys Acta* 1791:419–440. <https://doi.org/10.1016/j.bbali.2009.04.002>
- Brasaemle DL, Barber T, Wolins NE, Serrero G, Blanchette-Mackie EJ, Londos C (1997) Adipose differentiation-related protein is an ubiquitously expressed lipid storage droplet-associated protein. *J Lipid Res* 38:2249–2263
- Buechler C, Ritter M, Duong CQ, Orso E, Kapinsky M, Schmitz G (2001) Adipophilin is a sensitive marker for lipid loading in human blood monocytes. *Biochem Biophys Acta* 1532:97–104. [https://doi.org/10.1016/s1388-1981\(01\)00121-4](https://doi.org/10.1016/s1388-1981(01)00121-4)
- Chen YC, Chen CH, Hsu YH, Chen TH, Sue YM, Cheng CY, Chen TW (2011) Leptin reduces gentamicin-induced apoptosis in rat renal tubular cells via the PI3K-Akt signaling pathway. *Eur J Pharmacol* 658:213–218. <https://doi.org/10.1016/j.ejphar.2011.02.025>
- Diéguez C, Vazquez MJ, Romero A, López M, Nogueiras R (2011) Hypothalamic control of lipid metabolism: focus on leptin, ghrelin and melanocortins. *Neuroendocrinology* 94:1–11. <https://doi.org/10.1159/000328122>
- Eberlé D, Hegarty B, Bossard P, Ferré P, Foulfelle F (2004) SREBP transcription factors: master regulators of lipid homeostasis. *Biochimie* 86:839–848. <https://doi.org/10.1016/j.biochi.2004.09.018>
- Engelking LJ, Kuriyama H, Hammer RE, Horton JD, Brown MS, Goldstein JL, Liang G (2004) Overexpression of Insig-1 in the livers of transgenic mice inhibits SREBP processing and reduces insulin-stimulated lipogenesis. *J Clin Invest* 113:1168–1175. <https://doi.org/10.1172/jci20978>
- Forbes JM, Cooper ME (2013) Mechanisms of diabetic complications. *Physiol Rev* 93:137–188. <https://doi.org/10.1152/physrev.00045.2011>
- Furuichi K, Shimizu M, Hara A, Toyama T, Wada T (2018) Diabetic nephropathy: a comparison of the clinical and pathological features between the CKD Risk Classification and the Classification of Diabetic Nephropathy 2014 in Japan. *Internal medicine (Tokyo, Japan)* 57:3345–3350. <https://doi.org/10.2169/internalmedicine.1132-18>
- Girousse A, Gil-Ortega M, Bourlier V, Bergeaud C, Sastourné-Arrey Q, Moro C, Barreau C, Guissard C, Vion J, Arnaud E, Pradère JP, Juin N, Casteilla L, Sengenès C (2019) The release of adipose stromal cells from subcutaneous adipose tissue regulates ectopic intramuscular adipocyte deposition. *Cell Rep* 27:323–333. <https://doi.org/10.1016/j.celrep.2019.03.038>
- Grahame Hardie D (2016) Regulation of AMP-activated protein kinase by natural and synthetic activators. *Acta pharmaceutica Sinica B* 6:1–19. <https://doi.org/10.1016/j.apsb.2015.06.002>
- Hackl MT, Fürnsinn C, Schuh CM, Krssak M, Carli F, Guerra S, Freudenthaler A, Baumgartner-Parzer S, Helbich TH, Luger A, Zeyda M, Gastaldelli A, Buettner C, Scherer T (2019) Brain leptin reduces liver lipids by increasing hepatic triglyceride secretion and lowering lipogenesis. *Nat Commun* 10:2717. <https://doi.org/10.1038/s41467-019-10684-1>
- Hama H, Saito A, Takeda T, Tanuma A, Xie Y, Sato K, Kazama JJ, Gejyo F (2004) Evidence indicating that renal tubular metabolism of leptin is mediated by megalin but not by the leptin receptors. *Endocrinology* 145:3935–3940. <https://doi.org/10.1210/en.2004-0074>
- Han Y, Hu Z, Cui A, Liu Z, Ma F, Xue Y, Liu Y, Zhang F, Zhao Z, Yu Y, Gao J, Wei C, Li J, Fang J, Li J, Fan JG, Song BL, Li Y (2019) Post-translational regulation of lipogenesis via AMPK-dependent phosphorylation of insulin-induced gene. *Nat Commun* 10:623. <https://doi.org/10.1038/s41467-019-08585-4>
- Herman-Edelstein M, Scherzer P, Tobar A, Levi M, Gaftor U (2014) Altered renal lipid metabolism and renal lipid

- accumulation in human diabetic nephropathy. *J Lipid Res* 55:561–572. <https://doi.org/10.1194/jlr.P040501>
17. Hsu YH, Cheng CY, Chen YC, Chen TH, Sue YM, Tsai WL, Chen CH (2012) Long-term leptin treatment exerts a pro-apoptotic effect on renal tubular cells via prostaglandin E2 augmentation. *Eur J Pharmacol* 689:65–71. <https://doi.org/10.1016/j.ejphar.2012.06.008>
 18. Jun H, Song Z, Chen W, Zanhua R, Yonghong S, Shuxia L, Huijun D (2009) In vivo and in vitro effects of SREBP-1 on diabetic renal tubular lipid accumulation and RNAi-mediated gene silencing study. *Histochem Cell Biol* 131:327–345. <https://doi.org/10.1007/s00418-008-0528-2>
 19. Kang HM, Ahn SH, Choi P, Ko YA, Han SH, Chinga F, Park AS, Tao J, Sharma K, Pullman J, Bottinger EP, Goldberg IJ, Susztak K (2015) Defective fatty acid oxidation in renal tubular epithelial cells has a key role in kidney fibrosis development. *Nat Med* 21:37–46. <https://doi.org/10.1038/nm.3762>
 20. Kuwahara S, Hosojima M, Kaneko R, Aoki H, Nakano D, Sasagawa T, Kabasawa H, Kaseda R, Yasukawa R, Ishikawa T, Suzuki A, Sato H, Kageyama S, Tanaka T, Kitamura N, Narita I, Komatsu M, Nishiyama A, Saito A (2016) Megalin-mediated tubuloglomerular alterations in high-fat diet-induced kidney disease. *J Am Soc Nephrol* 27:1996–2008. <https://doi.org/10.1681/asn.2015020190>
 21. Li Y, Xu S, Mihaylova MM, Zheng B, Hou X, Jiang B, Park O, Luo Z, Lefai E, Shyy JY, Gao B, Wierzbicki M, Verbeuren TJ, Shaw RJ, Cohen RA, Zang M (2011) AMPK phosphorylates and inhibits SREBP activity to attenuate hepatic steatosis and atherosclerosis in diet-induced insulin-resistant mice. *Cell Metab* 13:376–388. <https://doi.org/10.1016/j.cmet.2011.03.009>
 22. Longo M, Zatterale F, Naderi J, Parrillo L, Formisano P, Raciti GA, Beguinot F, Miele C (2019) Adipose tissue dysfunction as determinant of obesity-associated metabolic complications. *Int J Mol Sci* 20(9):2358. <https://doi.org/10.3390/ijms20092358>
 23. Martínez-Sánchez N (2020) There and back again: leptin actions in white adipose tissue. *Int J Mol Sci* 21(17):6039. <https://doi.org/10.3390/ijms21176039>
 24. Mishra R, Emancipator SN, Miller C, Kern T, Simonson MS (2004) Adipose differentiation-related protein and regulators of lipid homeostasis identified by gene expression profiling in the murine db/db diabetic kidney. *Am J Physiol Renal Physiol* 286:F913–921. <https://doi.org/10.1152/ajprenal.00323.2003>
 25. Nielsen R, Christensen EI, Birn H (2016) Megalin and cubilin in proximal tubule protein reabsorption: from experimental models to human disease. *Kidney Int* 89:58–67. <https://doi.org/10.1016/j.kint.2015.11.007>
 26. Ouyang S, Mo Z, Sun S, Yin K, Lv Y (2020) Emerging role of Insig-1 in lipid metabolism and lipid disorders. *Clin Chim Acta* 508:206–212. <https://doi.org/10.1016/j.cca.2020.05.042>
 27. Palygin O, Spires D, Levchenko V, Bohovyk R, Fedoriuk M, Klemens CA, Sykes O, Bukowy JD, Cowley AW Jr, Lazar J, Ilatovskaya DV, Staruschenko A (2019) Progression of diabetic kidney disease in T2DN rats. *Am J Physiol Renal Physiol* 317:F1450–f1461. <https://doi.org/10.1152/ajprenal.00246.2019>
 28. Paz-Filho G, Mastroradi CA, Licinio J (2015) Leptin treatment: facts and expectations. *Metab. Clin. Exp* 64:146–156. <https://doi.org/10.1016/j.metabol.2014.07.014>
 29. Saravanan S, Pari L (2016) Protective effect of thymol on high fat diet induced diabetic nephropathy in C57BL/6J mice. *Chem Biol Interact* 245:1–11. <https://doi.org/10.1016/j.cbi.2015.11.033>
 30. Sehgal V, Ulmer B (2019) Clinical conundrums in the management of diabetic ketoacidosis in the elderly. *Journal of translational internal medicine* 7:10–14. <https://doi.org/10.2478/jtim-2019-0003>
 31. Su K, Yi B, Yao BQ, Xia T, Yang YF, Zhang ZH, Chen C (2020) Liraglutide attenuates renal tubular ectopic lipid deposition in rats with diabetic nephropathy by inhibiting lipid synthesis and promoting lipolysis. *Pharmacol Res* 156:104778. <https://doi.org/10.1016/j.phrs.2020.104778>
 32. Sun L, Halaihel N, Zhang W, Rogers T, Levi M (2002) Role of sterol regulatory element-binding protein 1 in regulation of renal lipid metabolism and glomerulosclerosis in diabetes mellitus. *J Biol Chem* 277:18919–18927. <https://doi.org/10.1074/jbc.M110650200>
 33. Tervaert TW, Mooyaart AL, Amann K, Cohen AH, Cook HT, Drachenberg CB, Ferrario F, Fogo AB, Haas M, de Heer E, Joh K, Noël LH, Radhakrishnan J, Seshan SV, Bajema IM, Bruijn JA (2010) Pathologic classification of diabetic nephropathy. *J Am Soc Nephrol* 21:556–563. <https://doi.org/10.1681/asn.2010010010>
 34. Vaziri ND (2016) Disorders of lipid metabolism in nephrotic syndrome: mechanisms and consequences. *Kidney Int* 90:41–52. <https://doi.org/10.1016/j.kint.2016.02.026>
 35. Walker AK, Jacobs RL, Watts JL, Rottiers V, Jiang K, Finnegan DM, Shioda T, Hansen M, Yang F, Niebergall LJ, Vance DE, Tzoneva M, Hart AC, Näär AM (2011) A conserved SREBP-1/ phosphatidylcholine feedback circuit regulates lipogenesis in metazoans. *Cell* 147:840–852. <https://doi.org/10.1016/j.cell.2011.09.045>
 36. Wang Q, Liu S, Zhai A, Zhang B, Tian G (2018) AMPK-mediated regulation of lipid metabolism by phosphorylation. *Biol Pharm Bull* 41:985–993. <https://doi.org/10.1248/bpb.b17-00724>
 37. Wang Z, Jiang T, Li J, Proctor G, McManaman JL, Lucia S, Chua S, Levi M (2005) Regulation of renal lipid metabolism, lipid accumulation, and glomerulosclerosis in FVBdb/db mice with type 2 diabetes. *Diabetes* 54:2328–2335. <https://doi.org/10.2337/diabetes.54.8.2328>
 38. Yang T, Espenshade PJ, Wright ME, Yabe D, Gong Y, Aebersold R, Goldstein JL, Brown MS (2002) Crucial step in cholesterol homeostasis: sterols promote binding of SCAP to INSIG-1, a membrane protein that facilitates retention of SREBPs in ER. *Cell* 110:489–500. [https://doi.org/10.1016/s0092-8674\(02\)00872-3](https://doi.org/10.1016/s0092-8674(02)00872-3)
 39. Yang W, Luo Y, Yang S, Zeng M, Zhang S, Liu J, Han Y, Liu Y, Zhu X, Wu H, Liu F, Sun L, Xiao L (2018) Ectopic lipid accumulation: potential role in tubular injury and inflammation in diabetic kidney disease. *Clin Sci (London, England : 1979)* 132:2407–2422. <https://doi.org/10.1042/cs20180702>
 40. Yu X, McCorkle S, Wang M, Lee Y, Li J, Saha AK, Unger RH, Ruderman NB (2004) Leptinomimetic effects of the AMP kinase activator AICAR in leptin-resistant rats: prevention of diabetes and ectopic lipid deposition. *Diabetologia* 47:2012–2021. <https://doi.org/10.1007/s00125-004-1570-9>
 41. Zeni L, Norden AGW, Cancarini G, Unwin RJ (2017) A more tubulocentric view of diabetic kidney disease. *J Nephrol* 30:701–717. <https://doi.org/10.1007/s40620-017-0423-9>
 42. Zhang Y, Proenca R, Maffei M, Barone M, Leopold L, Friedman JM (1994) Positional cloning of the mouse obese gene and its human homologue. *Nature* 372:425–432. <https://doi.org/10.1038/372425a0>

Publisher's note Springer Nature remains neutral with regard to jurisdictional claims in published maps and institutional affiliations.